Simultaneous and independent processing of multiple input WDM data signals using a tunable optical tapped delay line

Salman Khaleghi,[1,*] Mohammad Reza Chitgarha,[1] Morteza Ziyadi,[1] Wajih Daab,[1] Amirhossein Mohajerin-Ariaei,[1] Dvora Rogawski,[1] Joseph D. Touch,[2] Moshe Tur,[3] Carsten Langrock,[4] Martin M. Fejer,[4] and Alan E. Willner[1]

[1]*Department of Electrical Engineering, University of Southern California, Los Angeles, California 90089, USA*

[2]*Information Sciences Institute, University of Southern California, 4676 Admiralty Way, Marina del Rey, California 90292, USA*

[3]*School of Electrical Engineering, Tel Aviv University, Ramat Aviv 69978, Israel*

[4]*Edward L. Ginzton Laboratory, Stanford University, Stanford, California 94305, USA*

**Corresponding author: khaleghi@usc.edu*

Received July 29, 2013; accepted August 25, 2013;
posted September 19, 2013 (Doc. ID 194786); published October 17, 2013

We demonstrate a tunable optical tapped delay line that can simultaneously and independently operate on multiple wavelength-division multiplexed (WDM) data signals. The system utilizes the wavelength-dependent speed of light, together with nonlinear wavelength conversion stages. A phase-preserving scheme enables coherent addition of the weighted taps. We reconfigured the system to perform separate simultaneous correlation (data pattern recognition), equalization, and modulation format conversion on four and eight WDM binary/quadrate phase-shift keyed channels at 26 and 20 Gbaud, respectively. The aggregate throughput of 416 Gb/s is achieved.

OCIS codes: (060.2360) Fiber optics links and subsystems; (060.4370) Nonlinear optics, fibers; (190.4223) Nonlinear wave mixing.
http://dx.doi.org/10.1364/OL.38.004273

Optical signal processing techniques that make use of both the amplitude and phase information hold the potential to increase processing capacity by operating at the line rate of optical communications. The amount of data that can be processed in bit time can be dramatically increased by encoding information bits as multilevel phase and amplitude symbols (e.g., quadrature-amplitude-modulation [QAM] formats), using wavelength and polarization multiplexing, and utilizing higher symbol transmission rates (baud rate). A key building block for processing such complex encodings is the tapped delay line (TDL), in which an input signal is tapped at various time intervals, each tap is multiplied by a complex coefficient, and taps are finally added to create the output [1]. Complex-coefficient optical TDLs (OTDLs) have been shown to operate on the amplitude and phase of data signals to increase processing capacity [2]. OTDLs can be configured to perform different functions such as finite-impulse-response filtering [3], equalization, correlation [2,4], discrete Fourier transform (DFT) [5], and format conversion [6].

An OTDL equalizer based on a photonic integrated circuit has been demonstrated in [3] that can simultaneously process 16 wavelength-division multiplexed (WDM) channels. However, the tap delays were not widely tunable, and the same function was applied to all WDM channels. A baud-rate adjustable OTDL with tunable complex tap coefficients has been shown, which exploits nonlinear wave mixing and tunable optical delays [2]. Although this OTDL is tunable, it can only operate on a single wavelength channel.

In this Letter, we demonstrate a single OTDL system that can simultaneously and independently process multiple WDM data channels. The WDM-OTDL is baud-rate adjustable, and the number of WDM input channels can easily be scaled.

We exploit four-wave mixing (FWM) and three-wave mixing in nonlinear devices such as highly nonlinear fiber (HNLF) and periodically poled lithium niobate (PPLN), conversion–dispersion optical delay [7], and amplitude and phase programmable liquid crystal on silicon (LCoS) filters to realize concurrent independent functions on different WDM channels. We show a two-tap OTDL on four and eight WDM channels, to perform independent and reconfigurable equalization, two-symbol pattern recognition, and format conversion on binary phase shift keyed (BPSK) and quadrate phase shift keyed (QPSK) signals at 20 and 26 Gbaud. To demonstrate this capability, we show format conversion from BPSK to either QPSK or 4-PAM (pulse amplitude modulation), and from QPSK to 16-QAM. We also demonstrate parallel correlation on eight 20 Gbaud QPSK WDM signals with a data throughput of 416 Gb/s [8].

The concept of a WDM-OTDL is illustrated in Fig. 1. A set of WDM channels is input to the system, and as the signals propagate on the same path, the WDM-OTDL can concurrently perform independent functions on each channel. In Fig. 1, channel A is format converted from QPSK to 16-QAM, channel B is equalized, and a correlation is performed on channel C.

The fundamental building block of the WDM-OTDL is a two-tap OTDL that operates on WDM input channels, as depicted in Fig. 2. The principle of operation is shown in Fig. 2(a). The WDM input channels are simultaneously wavelength converted in a nonlinear medium, generating a replica for each WDM channel at a new center frequency. Because each signal and its replica are at different frequencies, a relative delay is induced between them

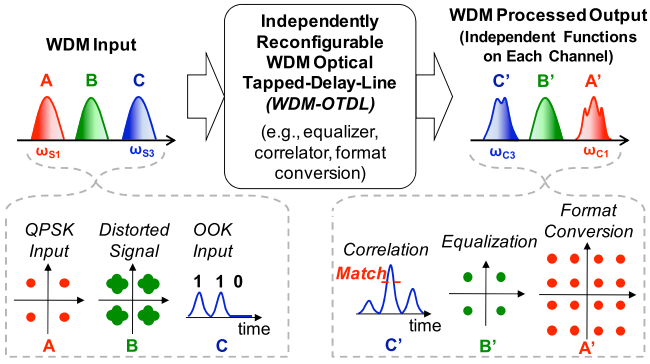

Fig. 1. Concept of independent processing of WDM channels in a WDM OTDL (showing format conversion on channel A, equalization on channel B, and correlation on channel C). OOK, on–off keying.

after passing through a chromatic dispersive medium. Here we assume the originals are delayed relative to the replicas (i.e., dispersion increases with frequency). The replicas and the delayed original signals are then sent into a phase and amplitude programmable filter based on LCoS technology that applies the complex tap coefficients to the replicas. Finally, the delayed original signals and their weighted replicas are sent into another wavelength converting stage that coherently copies the original signals onto the replicas for a second time, creating the desired two-tap processing. Thus, a same-delay though independent two-tap OTDL can be implemented on each WDM channel. The equivalent system diagram is shown in Fig. 2(b), in which a distinct tap coefficient is applied on each WDM channel. A higher number of taps can potentially be implemented by cascading the two-tap tunable building blocks, as in Fig. 3.

Figure 3 describes a three-tap processor and illustrates the nonlinear wave mixing for the wavelength converting stages as well as the dispersion delays for a three-tap implementation. In general, N WDM input signals with electric field amplitude $E_{\mathrm{Si}}(t)$ at center frequency ω_{Si} are considered ($i \in \{1, \ldots, N\}$). The WDM signals are combined with a continuous-wave (CW) pump E_P at frequency ω_P and are sent to a nonlinear medium to generate copies of the input signals. The pump and signal configurations need to satisfy the phase matching conditions for efficient nonlinear wave mixing [9,10]. The nonlinear medium can be an HNLF or a PPLN waveguide. In the case of an HNLF, the CW pump is located close to the zero-dispersion wavelength (ZDW) of the HNLF so that the phase matching conditions are met for efficient

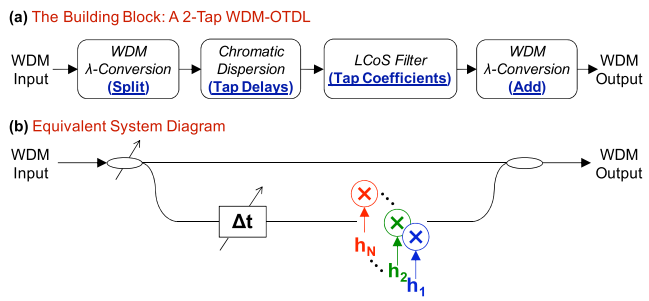

Fig. 2. Implementation of a two-tap OTDL as the building block of the WDM-OTDL: (a) block diagram and (b) equivalent system diagram.

degenerate FWM. If a PPLN waveguide is used instead, the CW pump must be located on the quasi-phase-matching (QPM) frequency of the waveguide to exploit the two cascaded second-order nonlinear processes of second harmonic generation followed by difference frequency generation (cSHG-DFG). The output of cSHG-DFG is similar to the degenerate FWM. Either implementation results in the generation of a wavelength-converted copy for each input signal at a new center frequency $\omega_{\mathrm{Ci}} = 2\omega_P - \omega_{\mathrm{Si}}$ with a field proportional to $E_{\mathrm{Ci}}(t) \propto E_P^2 E_{\mathrm{Si}}^*(t)$. The original data signals $E_{\mathrm{Si}}(t)$, the CW pump E_P, and the phase-conjugate signal copies $E_{\mathrm{Ci}}(t)$ are then sent to an LCoS filter. The LCoS filter applies a complex coefficient $|a_i|e^{\angle a_i}$ on each signal copy, making them proportional to $a_i E_{\mathrm{Ci}}(t)$. The CW pump, the signals, and the weighted copies are then sent to a dispersive device [e.g., a dispersion compensating fiber, (DCF)], in which signals at different frequencies propagate at different speeds. In a medium of length L and dispersion parameter D, a relative time delay of $T_i \approx DL(\lambda_{\mathrm{Si}} - \lambda_{\mathrm{Ci}})$ is induced between the original data signal and its copy. Note that because the CW pump is not data modulated, the relative time delay on the pump is equivalent to a phase shift and can be ignored. Next, the delayed signals $E_{\mathrm{Si}}(t - T_i)$ and the CW pump E_P mix in another PPLN waveguide and create another copy of the signal on the frequency of the first signal copy, proportional to $E_P^2 E_{\mathrm{Si}}^*(t - T_i)$. Therefore, the addition of the two signal copies at frequency ω_{Ci} is

$$E_{\mathrm{MUX},i}(t) \propto E_P^2 (E_{\mathrm{Si}}^*(t - T_i) + a_i E_{\mathrm{Si}}^*(t)), \tag{1}$$

representing a two-tap complex-value delay line processor.

This scheme can be adapted to large number of concurrent WDM signals without requiring extra nonlinear elements, and the delays can be varied by tuning the wavelength of the CW pump. As shown in Fig. 3, the number of taps can be increased by adding additional nonlinear stages, followed by a dispersive medium and an additional LCoS filter. In a more than two-tap situation, the final desired coefficients (a_1, b_1, etc.) must be properly scaled for correct final results (see Fig. 3). If the stages are cascaded, all coefficients must be nonzero, which is the case for many scenarios, e.g., DFT [5], correlation on PSK signals [2,4] and more. However, each additional nonlinear stage effectively reduces the overall signal-to-noise ratio, thereby limiting the maximum number of taps. For a reasonable number of taps (less than five), this scheme can dramatically increase the processing capacity per nonlinear device. For example, a k-tap OTDL on N wavelength channels using the scheme in [2] requires $2N$ nonlinear elements, whereas the proposed parallel processing WDM-OTDL design reduces this to k, making it a promising technique for cases requiring fewer taps and a higher number of wavelength channels (i.e., where $k < 2N$).

The experimental setup is depicted in Fig. 4. Eight CW lasers on a 100 GHz frequency grid are combined in a WDM coupler and sent to a nested Mach–Zehnder modulator that is driven by 20 and 26 Gbaud electrical data to generate either BPSK or QPSK signals. The WDM channels are then amplified and decorrelated using a demultiplexing stage followed by various optical delays.

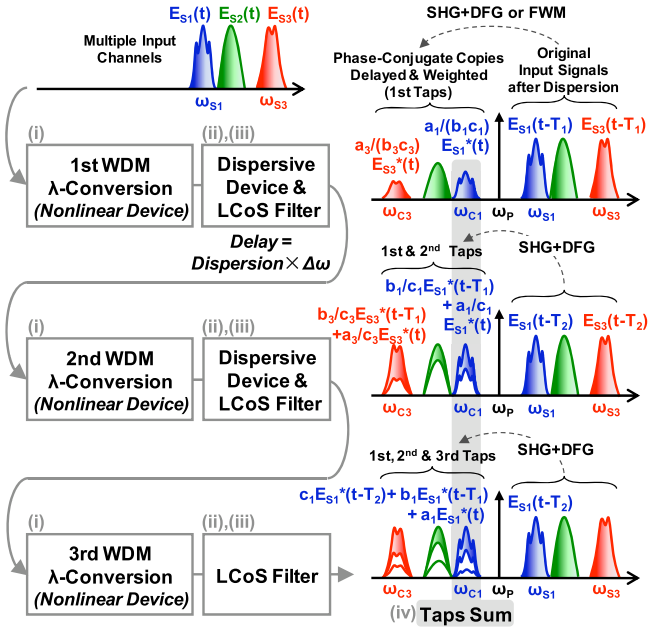

Fig. 3. Principle of operation of the WDM-OTDL, shown for a three-tap implementation: (i) taps are created by simultaneous wavelength conversion of all WDM channels in nonlinear elements, with one such element for each tap. (ii) Due to the large wavelength difference (~10 nm) between each signal and its replica, a dispersive element induces a relative delay between them. (iii) Tap coefficients are applied by an inline LCoS filter. (iv) Because the pumps are reused, the weighted taps add coherently. The number of taps is the number of nonlinear wavelength converting stages.

A phase and amplitude programmable filter based on LCoS technology is used for demultiplexing. The LCoS filter can also distort a channel by applying a chromatic dispersion (CD) of 200 ps/nm for the equalization experiment. The WDM signals and a ~1551/1551.6 nm CW pump are then amplified separately in erbium-doped-fiber amplifiers (EDFAs) and filtered and coupled into either a low-dispersion-slope ~200 m HNLF (ZDW ~1560 nm) or a 4 cm PPLN waveguide. The HNLF is used

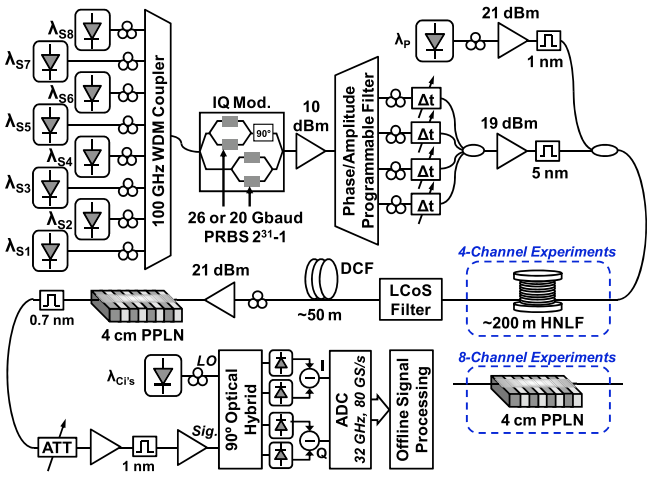

Fig. 4. Experimental setup for two experiments: a four-channel WDM-OTDL using an HNLF as the wavelength conversion medium and an eight-channel operation using a PPLN waveguide instead of the HNLF. IQ, in-phase and quadrature; PRBS, pseudo-random bit sequence; ATT, variable optical attenuator.

for four-channel experiments at 26 Gbaud, and the PPLN is used for eight-channel experiments at 20 Gbaud. The output is then sent into an LCoS filter that applies the tap coefficients. All weighted signals and pumps then travel through ~50 m DCF to induce the tap delays. The LCoS filter also (i) adjusts the relative time delays between the original signals and their copies, such that only one (two) symbol time delay is induced between the closer (farther) four WDM channels, and (ii) balances the relative power of the CW pump and the signals to equalize the various EDFA gain profiles and conversion efficiencies. All signals are then amplified and sent to another 4 cm PPLN waveguide to create the second copies. For eight-channel 20 Gbaud experiments, the QPM wavelengths of both PPLN waveguides are thermally tuned up from 1551 to ~1551.6 nm such that the single-symbol delays are changed from ~38 ps (26 Gbaud) to 50 ps (20 Gbuad). Each wavelength-converted signal copy is then filtered and detected coherently using a local oscillator, 90° optical hybrid, and analog-to-digital converters (ADCs) to measure error vector magnitude (EVM) and bit error ratio (BER) by offline processing.

Figure 5(a) depicts the spectra of the HNLF and PPLN output for the four-channel 26 Gbaud QPSK experiments. The two-tap OTDL is, in principle, an interferometer, and thus destructive interference can be observed as power dips in the converted signals of the PPLN output

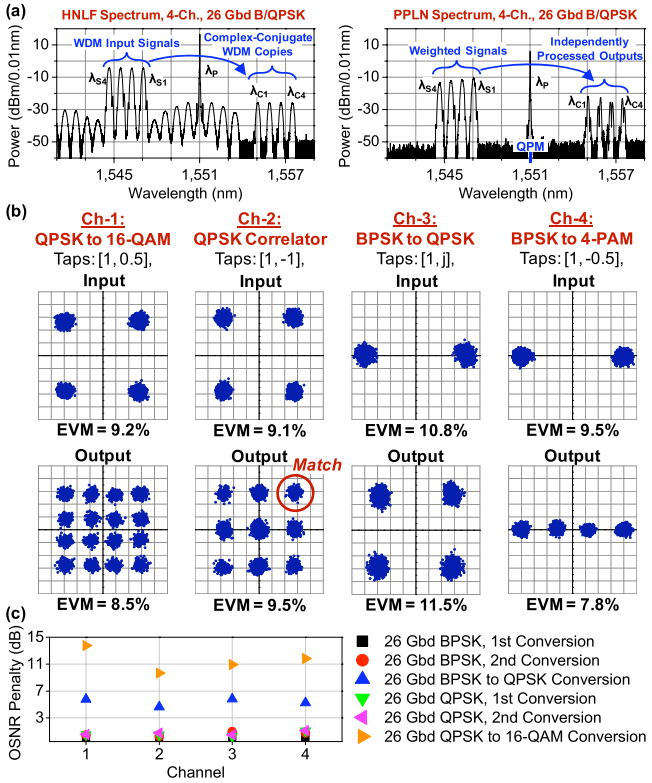

Fig. 5. Four 26 Gbaud BPSK/QPSK WDM channels using an HNLF as the first nonlinear stage and a PPLN as the second: (a) optical spectra after the HNLF and the PPLN device, showing the first and second set of taps, respectively, (b) input and output constellation diagrams for various modulation formats and independent functions on different channels, and (c) OSNR penalty of each tap (conversion) and format conversion for BPSK to QPSK and QPSK to 16-QAM.

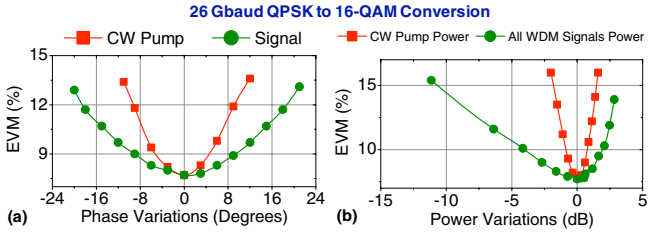

Fig. 6. Sensitivity of the system to (a) phase and (b) power variations for QPSK to 16-QAM conversion on channel 4.

spectrum. Different spectral shapes are due to the particular functions implemented by varying the tap coefficients. Examples of various independent and tunable functions on the four WDM channels are shown in Fig. 5(b). Correlation for a two-symbol pattern search and format conversion from BPSK/QPSK to 4-PAM/16-QAM are performed by applying various tap coefficients, as noted in Fig. 5(b). In Fig. 5(c), the optical signal-to-noise ratio (OSNR) penalties at BER $= 2 \times 10^{-3}$ are shown for the first and second wavelength conversion stages, as well as for modulation format conversion. The format-converted QPSK signal, for example, has <7 dB OSNR penalty compared to a back-to-back BPSK measurement (i.e., <1 dB penalty compared to back-to-back QPSK).

All signals, as well as the CW pump, are amplified in a single constant-power EDFA before the second nonlinear stage. As a result, a change of either phase or power in one of the amplified waves may affect the other. Figure 6 characterizes this sensitivity. Conversion of 26 Gbaud QPSK to 16-QAM on channel 4 is evaluated. The phases of all WDM signals and the CW pump are varied in the LCoS filter before the second nonlinear stage, and the powers are varied by changing the power of the two EDFAs on the WDM input signals and the CW pump. As can be seen in Fig. 6(a), the output is twice as sensitive to the phase variations of the CW pump compared to variations of the input signal. This difference in sensitivity occurs because the second tap is proportional to the square of the CW pump field, but proportional to the signal fields. For the same reason, the output is more sensitive to power variations in the CW pump than to variations of the signals [Fig. 6(b)]. Additionally, increasing the CW power deteriorates the output signal more than decreasing it, possibly due to extra phase shift from self-phase modulation inside the HNLF.

The use of HNLF in the first stage creates multiple parasitic mixing terms due to nondegenerate FWM between the signals and the pump, which consume bandwidth. However, if cSHG-DFG in a PPLN device is used instead of degenerate FWM in the first stage, then more channels can be processed. Figure 7(a) depicts the spectra of the two PPLN outputs for eight-channel 20 Gbaud QPSK input signals. In Fig. 7(b), the input channel-1 is distorted by 200 ps/nm CD before the first stage and is equalized using a two-tap half-symbol time equalizer with appropriate tap coefficients. The figure also shows the input and output constellation diagrams. The system is reconfigured to perform eight parallel two-symbol correlations on 20 Gbaud QPSK data signals with various target patterns to achieve a throughput of 416 Gb/s [as shown in Fig. 7(c)]. Because the eight signals span a wide spectral range, the LCoS filter is unable to correct for the resulting large variations of the signals' wavelength-dependent delays. Therefore, we

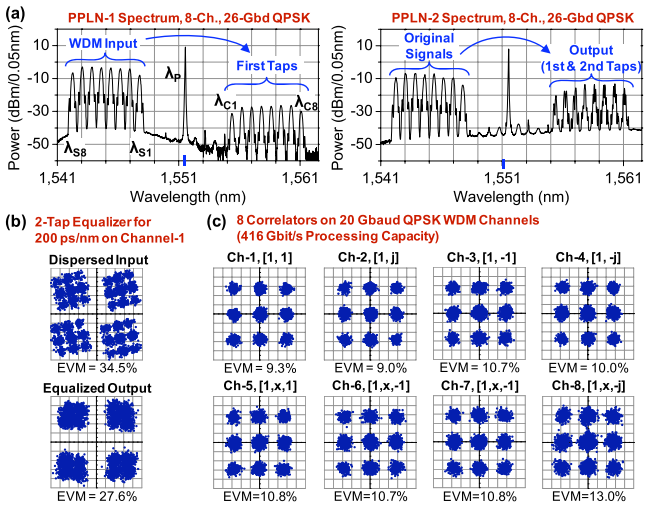

Fig. 7. Eight 20 Gbaud QPSK WDM channels using a PPLN waveguide in the first stage: (a) spectra after the first and the second nonlinear stages, (b) A two-tap equalizer for a signal that is distorted by 200 ps/nm CD, and (c) simultaneous two-symbol pattern search on eight WDM channels, resulting in an aggregate throughput of 416 Gb/s.

chose tap delays of two symbol time for the farther four channels. In general, if one bit delay is required, one may use a lower baud rate on farther channels and a higher baud rate on channels closer to the center frequency.

This work is partially supported by the NSF, NSF Center for Integrated Access Networks (CIAN) under contract 0812072, DARPA, and Cisco Systems.

References

1. J. G. Proakis, *Digital Communications* (McGraw-Hill, 2000).
2. S. Khaleghi, O. F. Yilmaz, M. R. Chitgarha, M. Tur, N. Ahmed, S. R. Nuccio, I. M. Fazal, X. Wu, M. W. Haney, C. Langrock, M. M. Fejer, and A. E. Willner, IEEE Photon. J. **4**, 1220 (2012).
3. C. R. Doerr, S. Chandrasekhar, P. J. Winzer, A. R. Chraplyvy, A. H. Gnauck, L. W. Stulz, R. Pafchek, and E. Burrows, J. Lightwave Technol. **22**, 249 (2004).
4. I. Kang, M. Rasras, M. Dinu, M. Cappuzzo, L. T. Gomez, Y. F. Chen, L. Buhl, S. Cabot, A. Wong-Foy, S. S. Patel, C. R. Giles, N. Dutta, J. Jaques, and A. Piccirilli, IEEE Photon. Technol. Lett. **20**, 1024 (2008).
5. D. Hillerkuss, R. Schmogrow, T. Schellinger, M. Jordan, M. Winter, G. Huber, T. Vallaitis, R. Bonk, P. Kleinow, F. Frey, M. Roeger, S. Koenig, A. Ludwig, A. Marculescu, J. Li, M. Hoh, M. Dreschmann, J. Meyer, S. Ben Ezra, N. Narkiss, B. Nebendahl, F. Parmigiani, P. Petropoulos, B. Resan, A. Oehler, K. Weingarten, T. Ellermeyer, J. Lutz, M. Moeller, M. Huebner, J. Becker, C. Koos, W. Freude, and J. Leuthold, Nat. Photonics **5**, 364 (2011).
6. S. Khaleghi, M. R. Chitgarha, O. F. Yilmaz, M. Tur, M. W. Haney, C. Langrock, M. M. Fejer, and A. E. Willner, Opt. Lett. **38**, 1600 (2013).
7. Y. Dai, Y. Okawachi, A. C. Turner-Foster, M. Lipson, A. L. Gaeta, and C. Xu, Opt. Express **18**, 333 (2010).
8. S. Khaleghi, M. R. Chitgarha, M. Ziyadi, W. Daab, A. Mohajerin-Ariaei, D. Rogawski, J. D. Touch, M. Tur, C. Langrock, M. M. Fejer, and A. E. Willner, in *Optical Fiber Communication Conference* (2013), paper OTh4D.2.
9. C. Langrock, S. Kumar, J. E. McGeehan, A. E. Willner, and M. M. Fejer, J. Lightwave Technol. **24**, 2579 (2006).
10. G. Agrawal, *Nonlinear Fiber Optics* (Academic, 2001).